Published in final edited form as:
*Biomater Sci*. 2014 ; 2: 1779–1786. doi:10.1039/C4BM00164H.

# Stable biofunctionalization of hydroxyapatite (HA) surfaces by HA-binding/osteogenic modular peptides for inducing osteogenic differentiation of mesenchymal stem cells†

**Alessandro Polini**[a,‡], **Jianglin Wang**[b], **Hao Bai**[a], **Ye Zhu**[b], **Antoni P. Tomsia**[a], and **Chuanbin Mao**[a,b]

Alessandro Polini: alessandro.polini@radboudumc.nl; Chuanbin Mao: cbmao@ou.edu

[a]Materials Sciences Division, Lawrence Berkeley National Laboratory, Berkeley, CA 94720, USA

[b]Department of Chemistry and Biochemistry, Stephenson Life Sciences Research Center, University of Oklahoma, Norman, OK 73019, USA

## Abstract

Hydroxyapatite (HA), the principal component of bone mineral, shows osteoconductive properties when employed for coating metal implants as well as scaffold materials in synthetic bone grafts. With the goal of providing this material with osteoinductive capabilities to promote faster bone regeneration, we show an easy approach to functionalize HA implant surfaces and enrich them with osteoinductive properties by the use of HA-binding modular peptides. The modular peptides are designed as a combination of two domains, an HA-binding peptide motif and an osteogenic peptide motif derived from the osteogenic growth peptide (OGP) or bone morphometric protein 7 (BMP-7). To identify the best HA-binding peptide, several nature-inspired peptides derived from natural bone extracellular matrix proteins (bone sialoprotein, osteonectin, osteocalcin, and salivarin statherin) were compared for HA-binding activity, revealing concentration-dependent and incubation-time-dependent behaviours. We discovered that a Poly-E heptamer (E7) is the best HA-binding peptide, and thus combined it with a second osteogenic peptidic domain to create an osteoinductive modular peptide. After binding/release characterization, we found that the addition of the second osteogenic peptide domain did not change the binding profile of the modular peptides and caused only a slight change in their release kinetics. Mesenchymal stem cells (MSCs) were cultured on the HA substrates functionalized with modular peptides, and cell adhesion, proliferation, and differentiation in a basal medium (i.e., without any osteogenic supplements) were investigated. Gene expression data clearly showed that MSCs were committed to differentiate into osteoblasts in the presence of the modular peptides. HA discs functionalized with the E7 BMP-7 modular peptide showed the best capability in inducing the osteogenic differentiation of MSCs among all modular peptides studied. The modular peptides can easily be used to functionalize the HA implants through its constituent HA-binding motif, leaving the osteogenic peptide motif protruding from the surface for inducing osteogenesis. Our work opens

†Electronic supplementary information (ESI) available: Primer sequences for real-time PCR analysis; fluorescent images of peptide-functionalized HA surfaces. See DOI: 10.1039/c4bm00164h



Correspondence to: Alessandro Polini, alessandro.polini@radboudumc.nl; Chuanbin Mao, cbmao@ou.edu.
‡Present address: Department of Biomaterials, Radboud University Medical Center, 6525EX Nijmegen, The Netherlands.

up a new approach to the formulation of new bioactive HA coatings and implants for bone and dental repair.

## Introduction

Tissue-engineering strategies have been investigated for more than two decades for the repair or replacement of lost or damaged tissues due to birth defects, diseases, or accidents.[1] In this regard, scientists have dedicated significant research efforts to develop relatively inert (biotolerant) implants, which are useful as bare structural supports for cell growth and tissue remodelling, while minimizing graft-*versus*-host reactions (immune and fibrotic responses). The field has since matured, and currently focuses on the biology of these implants and on how cells, matrices, and inductive stimuli from the stem-cell niche affect cell fate.[1,2] Investigators have explored new pathways to produce materials able to interact with local tissues/cells and positively alter the endogenous healing processes by triggering cell-specific responses at the molecular level and by promoting better scaffold integration with surrounding tissues.[3] Modification of material physical properties (*e.g.*, elasticity and topography) as well as delivery of specific bio- molecules (*e.g.*, growth factors) are subjects of intensive scientific inquiry for the development of new scaffolds, which are intrinsically able to guide lineage-specific differentiation of stem cells.[2] In the wake of pioneering work in 2004 by McBeath *et al.*,[4] several groups investigated different approaches to direct and influence stem-cell differentiation toward specific lineages without exogenous supplements or any mechanical and external forces.[5–13]

For bone tissue, one of the most studied in tissue engineering, we witnessed the development of bioactive glasses, ceramics, glass-ceramics, and composites, which are now used routinely by clinicians for orthopedic and dental applications.[14,15] Because of its composition and structural similarity to natural bone, as well as its unique functional properties, hydroxyapatite (HA) is the implant material most commonly used in clinics today, even though its osteoinductive properties are still under debate and often limited to specific formulations.[16,17] Improvement of HA-based materials as suitable alternatives to autologous grafts remains a challenge in biomaterials research.

To produce intrinsically osteoinductive HA-based materials, we designed and characterized small modular peptides to engineer HA surfaces. Their osteoinductive properties were tested *in vitro* in the absence of osteogenic supplements. These peptides display two different domains: one serves as a binding site for the peptide to bind to the HA surface, similar to the natural mechanism by which bone extracellular matrix proteins bind HA (*i.e.*, electrostatic interactions); the second domain triggers specific cell responses at the molecular level and promotes osteogenic differentiation of mesenchymal stem cells (MSCs). We first compared three well-known HA-binding sequences (Table 1), including a Poly-Glu sequence,[18,19] present in osteonectin and bone sialoprotein; a sequence derived from osteocalcin;[20] and a sequence derived from salivary statherin.[21] We investigated the kinetics of their binding to and release from HA surfaces, and then chose the most effective sequence as an HA-binding domain in the design of modular peptides (Fig. 1). Later, we designed three modular peptides, sharing the same most effective HA-binding domain, but having a different second

domain, and tested them for their binding and release properties. These peptides were allowed to functionalize the HA surfaces by binding to HA through the HA-binding motif. Finally, we studied *in vitro* the effects of functionalized HA surfaces on the adhesion and proliferation of MSCs, as well as their differentiation toward the osteogenic lineage.

## Materials and methods

### Materials

All the peptides used in this work were obtained from American Peptide Company (Sunnyvale, CA). For the study of the kinetics of the peptide binding and release, C-terminal FITCtagged lyophilized peptides were purchased from the same company. HA powders (1–3 μm) were provided by Trans-Tech (Adamstown, MD). Rat MSCs were isolated from bone marrow of the rats following our published protocol.[22] Low-binding tubes (LoBind, Eppendorf, Hauppauge, NY) and pipette tips (VWR Signature, VWR, Visalia, CA) were employed during the functionalization and binding/release experiments in order to minimize the non-specific peptide adhesion on the plastic surfaces.

### HA disc preparation and functionalization

HA powder was pressed into disks using 0.25 in/0.5 in hardened steel-pressing dies under 3000 psi.[23] After sintering,[24] HA disks were stored in a vacuum desiccator at room temperature until use. For binding tests, HA disks were allowed to interact with FITC-peptides dissolved in phosphate-buffered solutions (PBS) at different concentrations (5–50 μM) for 24 h. The discs were also incubated in 50 μM FITC-peptide PBS solution for different incubation times (0.5–72 h). Release tests were carried out on the HA discs functionalized by incubation in 50 μM FITC-peptide PBS solution for 72 h. The same procedure was followed for preparing functionalized HA discs for cell-culture studies. The incubation was performed at room temperature using an orbital shaker (800 rpm). After functionalization, each sample was washed three times with PBS for 10 min. All the tests were carried out in triplicate, and un-functionalized disks were used as controls.

The presence and quantification of the peptide onto the HA surface were assessed by measuring the residual fluorescence of the solution (excitation: 495 nm; emission 520 nm) using a Gemini EM fluorescence microplate reader (Molecular Devices, Sunnyvale, CA) and comparing this emission to standard samples with known concentrations of FITC-labelled peptides. Additionally, functionalized discs were visualized using a fluorescent stereomicroscope (Olympus, Norcross, GA), using 1.5 s as the exposure time. For a semi-quantitative analysis, acquired images were analysed using image analysis software (Image J, NIH). A round region of interest, overlapping the disc surface, was selected and the mean intensity value and its standard deviation were determined for each image.

### Scanning electron microscopy (SEM)

The morphological characterization of modular peptides assembled on the scaffolds was observed by SEM. The peptide-coated scaffolds were briefly rinsed by PBS and then air-dried overnight in the hood. The dry specimens were subsequently sputter-coated with gold for characterization by SEM (NEON FEG-SEM, Zeiss, Thornwood, NY).

### Cell culture: adhesion and proliferation studies

Rat MSCs were cultured and expanded by our reported protocol.[25] Briefly, the MSCs were cultured in the basal medium that contained the Dulbecco's modified Eagle's media (DMEM, Gibco, Life Technologies), 15% foetal bovine serum (FBS, Gibco), and 1% antibiotics (penicillin 100 U $mL^{-1}$, streptomycin 100 U $mL^{-1}$). Prior to cell seeding, the peptidemodified HA discs were incubated in the basal medium for 10 days to remove the peptides released from discs and then transferred to a new 24-well culture plate for cell seeding. The MSCs at their third passage were seeded onto the scaffolds with a density of 5 × $10^5$ cells per scaffolds. The cell–scaffold composites were co-cultured in the basal medium for two weeks and the medium was replaced twice a week.

Adhesion of resident MSCs on the scaffolds was observed by confocal microscopy (Leica SP8, Leica Microsystems, Buffalo Grove, IL). At the designated time points of Day 3 and Day 5, the resident MSCs were rinsed by PBS three times and fixed with 4% paraformaldehyde at 4 °C for 30 min. They were permeabilized using 0.3% Triton X-100 for 5 min and then blocked with 5% goat serum solution for 1 h at room temperature. After blocking, the cellular F-actin and nuclei were stained by FITC-labeled phalloidin and DAPI, respectively.

For investigating the status of cell growth on the scaffolds, the cell proliferation was measured by 3-(4,5-dimethylthiazol- 2-yl)-2,5-diphenyl tetrazolium bromide (MTT, Sigma-Aldrich, St. Louis, MI) staining at the designated time points including Day 1, Day 3, Day 5, and Day 7. The cell-scaffold complex was incubated in the MTT solution (150 μL, 5 mg $mL^{-1}$) at 37 °C in a 5% $CO_2$ incubator for 4 h. The intense purple formazan derivative formed *via* cell metabolism was eluted and dissolved in 500 μL dimethylsulfoxide (DMSO, Sigma) per well. The absorbance was measured at 490 nm on a plate reader (BioTek, Winooski, VT).

### Cell culture: differentiation studies

Real-time polymerase chain reaction (PCR) analysis was performed using an Ambion Power SYBR Green cells-to-Ct Kit (Invitrogen) after two weeks of cell culture in the basal medium. The template cDNA was amplified with real-time quantitative PCR using primers of osteogenic specific genes including alkaline phosphatase (ALP), osteocalcin (OCN), osteopontin (OPN), and runt-related transcription factor 2 (Runx2).[13,26] Acidic ribosomal phosphoprotein (Arbp) was used as a reference gene. Sequences of the primers in this study are shown in Table S1.† The real-time PCR assay was done using the following protocol: initial denaturation at 95 °C for 5 min and 45 cycles of PCR (95 °C for 30s, 58 °C for 30 s, and 72 °C for 45 s). The assay was carried out in triplicate and relative gene expression was calculated with respect to the gene expression in the control substrate without any peptide coating.

## Results

### Binding/release studies of HA-binding peptide domains

To obtain a simple two dimensional (2-D) model for our experiments, we fabricated HA discs (1.5 mm thick, 5 mm in diameter for the binding/release tests; 3 mm thick, 10 mm in diameter for cell-culture studies).[23,27] To mimic the natural mechanism by which human bone extracellular matrix proteins bind HA, we chose a Poly-Glu sequence (termed E7),[18,19] present in osteonectin and bone sialoprotein; a sequence (termed OCN) from osteocalcin;[20] and finally a sequence (termed N15) from salivary statherin,[21] as shown in Table 1. To quantify the peptides bound to HA surfaces, we used FITC-labelled peptides and read the fluorescent signal of the peptide solution before and after incubation with the sample (*i.e.*, obtaining the exact amount of immobilized peptides by depletion).[20] E7 and OCN peptides showed a similar dosedependent behaviour, having ≈55 μmol $m^{-2}$ as a peak value at 50 μM, and did not reach a saturation point at the concentration range investigated (Fig. 2a). An N15 peptide clearly had a lower affinity toward our HA samples, showing values lower than 10 μmol $m^{-2}$ under all experimental conditions. After investigating the incubation time, we obtained the highest amount of E7 and OCN peptide molecules on the surface, equal to ≈60 μmol $m^{-2}$, after 48 h with no significant changes at longer times (Fig. 2b). For N15, the highest amount of immobilized molecules (≈7.5 μmol $m^{-2}$) was reached after only a few hours. Moreover, we performed a semi-quantitative study by analysing fluorescent images of the sample surface (Fig. S1 †), which confirmed the results from the depletion method (Fig. 2c, d). Similar trends in terms of binding properties at different peptide concentrations were found as well as at different incubation times. The analysis of the release kinetics over one month (Fig. 2e) indicates that E7 is the most promising peptide, showing a low burst release effect and preserving over 75% of the immobilized molecules (46.5 μmol $m^{-2}$). The OCN peptide experienced a higher burst release effect, and consequently, there was a lower amount of peptides remaining on its surface (≈30%, *i.e.*, 18.5 μmol $m^{-2}$). The N15 peptide had the lowest amount of molecules remaining on its surface after one month (7.1 μmol $m^{-2}$) or around 75% of the immobilized amount. These results were qualitatively confirmed by fluorescent microscopy (Fig. S2 †). To have a sustained presence of peptides that may influence long-term processes for tissue morphogenesis, we consequently selected E7 as the HA-binding peptide domain for further studies.

### Binding/release studies of modular peptides

In order to provide HA surfaces with biologically active molecules, we designed modular peptides by adding to the HA binding domain E7 a second osteogenic domain, chosen from two well-known osteogenic molecules, including osteogenic growth peptide (OGP) and bone morphogenic protein 7 (BMP-7), involved in bone formation (Table 1). The resulting modular peptides are termed E7 OGP and E7 BMP-7, respectively. We also designed a third modular sequence, termed E7 polyG, where the second osteogenic domain in the modular peptide was replaced with a non-osteogenic polyG motif as a control (Table 1). We used both the depletion method and image analysis to test the binding kinetics of the three modular peptides, and did not find obvious differences among the three modular peptides (Fig. 3a–d) because they all shared the same HA-binding E7 peptide domain. Moreover, the addition of the second domain did not affect the binding properties of the HA-binding E7

peptide domain, as E7 OGP, E7 BMP-7 and E7 Poly-G showed a behaviour similar to that of E7. The analysis of the release kinetics showed that about 60% (36 μmol $m^{-2}$) of the modular peptides were still attached to the surface after one month (Fig. 3e), although this value is lower than the amount related to the E7 sequence alone (≈75%). These results were also qualitatively confirmed by fluorescence microscopy (Fig. S4 †). Overall, our findings affirm that the addition of a second domain only slightly affects the release of the whole peptide from the surface. These studies confirmed that the modular peptides were immobilized on the HA discs by binding to HA through their HA-binding E7 domain.

### Cell culture study

Prior to investigating the cell behaviour on the modular peptide-functionalized HA substrates, we performed a morphological characterization of their surfaces by SEM. We observed clear differences upon functionalization, with all the peptides forming self-assembled structures with microscale features (Fig. 4). As a control, bare HA samples were incubated in PBS and no regular structure was observed on the surface.

We proceeded to investigate the behaviour of resident MSCs on the biofunctionalized HA substrates. The data demonstrated that all materials exhibited high biocompatibility and strongly supported cell adhesion. After three days, the blank control group showed the highest cell density whereas E7 Poly-G showed the lowest cell density and the E7 OGP group showed slightly more cells than the E7 BMP-7 group (Fig. 5a). Therefore, although all materials were able to promote cell attachment and growth, there was a significant difference in the cell number between various peptide-coated materials. In addition, the groups with peptide modification were less fibroblast-like than the blank control group. After seven days, no major changes were found in cell morphology for each group (Fig. 5b). Based on the results from the proliferation tests (Fig. 5c), both blank control and E7 Poly-G showed an increase in cell number from Day 1 to Day 7. The groups of E7 OGP and E7 BMP-7 also showed an increased cell number initially, from Day 1 to Day 5, but a slight decrease from Day 5 to Day 7.

Further investigation of cell differentiation induced by substrate materials was verified by gene expression analysis of osteogenic-specific markers (ALP, OCN, OPN, Runx2) after two weeks of culture in a basal medium without any osteogenic supplements. Real-time PCR analysis demonstrated that the material groups of E7 OGP and E7 BMP-7 had significantly higher mRNA levels of OCN, OPN, and Runx2 genes when compared to blank control and E7 Poly-G. The E7 BMP-7 group shows even a higher level of the osteogenicspecific genes than the E7 OGP group (Fig. 6). Namely, the E7 BMP-7 functionalized samples significantly enhanced osteogenic gene expression and promoted osteogenesis among all substrates studied.

## Discussion

The complex architecture of bones and teeth includes a combination of hard tissues (*i.e.*, compact and trabecular bone or enamel, dentin, and cementum) and soft tissues (*i.e.*, bone marrow or dental pulp, and periodontal ligament). The accurate organization of these two components makes these tissues hard to replicate and substitute. Conventional hard

materials, such as ceramics and metals, usually employed in bone implants, fail indeed in replicating all the biological cues necessary to trigger proper bone regeneration. The possibility of surface functionalization of ceramic materials in an effective way for influencing stem cell differentiation and bone development can open the way to more performing bone implants. Looking at nature, small peptide sequences (8–15 amino acids long) present in acidic, calcium-binding bone extracellular matrix proteins (*i.e.* sialoprotein, osteocalcin, and salivary statherin) are known to bind strongly to bone mineral surfaces. These sequences are enriched in acidic amino acid residues, which facilitate the coordination of calcium ions in a spatial orientation complementary to calcium ions in a hydroxyapatite crystal lattice.[28–31] Sequences from osteonectin and bone sialoprotein (E7), osteocalcin (OCN) and salivary statherin (N15) were capable of binding to calcium phosphatebased materials such as HA powder,[18,20,32] slabs,[20,32] discs,[19,23,27] HA–Ti implants,[33] β-TCP granules,[34] *in vitro* grown HA layers,[32] native bone grafts,[35] and allografts.[36] However, no clear results or direct comparison of surface binding and release properties between these different HA binding domains have been reported. Using fluorescent tags, we confirmed that these sequences bind HA surfaces with different affinities, but show a dose-dependent behaviour and a different binding/release profile. Our work also shows that E7 is the best HA-binding peptide among the three peptides studied. Thus, we used E7 as the HA-binding motif in the design of a modular peptide that can bind to HA through one end and also bear an osteogenic peptide domain at the other end.

To improve the osteogenic properties of HA materials that make them useful as bone implants, we designed modular peptides by combining the HA-binding E-7 peptide motif with a second osteogenic domain enabling them to positively affect the osteogenic differentiation process of MSCs. By exploiting the HA-binding properties of the first domain, large amounts of peptides could be maintained *in situ* (*i.e.*, on the surface of HA materials) making this approach an advantageous alternative to the administration of recombinant human proteins: immunogenicity problems due to systemic circulation can be overcome and denaturation/degradation by circulating enzymes can be reduced.[36] We chose the second domain from two well-known molecules involved in bone formation and designed a third sequence as a control. The first was OGP, a 14-mer growth factor peptide found in serum at μmol $L^{-1}$ concentrations, which is able to regulate proliferation, differentiation, and matrix mineralization in osteoblast lineage cells.[22,37] The second was BMP-7, an important protein involved in several biological processes and able to promote osteogenic differentiation and proliferation during new bone generation.[38] In the control sequence (E7 Poly-G), we added a polyglycine tail to the E7 sequence. All these peptides carried a proline residue at the junction to promote the turn of the sequence away from the surface—as proposed by Gilbert *et al.*[21] Interestingly, the addition of the second domain to the HA-binding domain did not affect its binding properties and no differences were found among the different modular peptides in terms of binding and release profiles. These peptides had great affinity towards HA surfaces over time (≈60% left on the surface after one month), although lower than using just the E7 sequence alone (≈75%).

SEM investigation clearly showed differences in the peptide self-assembling properties. All the peptides formed self-assembled structures with micro-/nano-scale features. The E7 OGP

peptide co-precipitated with PBS, forming porous structures in a manner similar to those reported in the literature for calcium phosphate surfaces (Fig. 4).[39] The E7 BMP-7 peptide exhibited plate-like, sharp edges and well-crystallized morphologies, which are typical of calcium phosphate mineral coatings.[40] E7 Poly-G, the control modular peptide sequence, showed a slightly different microstructure. The incubation of bare HA samples in PBS did not lead to any regular structure. Though these peptides shared the same “anchor” to bind HA, they showed different morphologies. Further experiments will be performed to study these differences in greater depth.

To verify that these modular peptides assembled on the substrate surface can further regulate the resident stem cell fate, HA surfaces functionalized with modular peptides were investigated *in vitro*. All the samples showed good cytocompatibility properties, allowing a strong cell adhesion and growth. Small differences were found in cell morphology and cell number, with E7 OGP and E7 BMP-7 showing a broader cell shape and lower proliferation rate (Fig. 5). These differences might be correlated with the difference in cell differentiation among these groups (Fig. 6), as stem cells tend to modify their cytoskeleton organization and decrease their proliferation upon differentiation.[41] This hypothesis was confirmed by gene expression analysis of osteogenic-specific markers, such as ALP, OCN, OPN, Runx2 (Fig. 6). These genes are overexpressed during the matrix maturation and at the onset of mineralization that follows the first phase of cell proliferation, and are considered markers of osteogenesis.[41]

The material group of E7 BMP-7 demonstrated the highest levels of overexpression of these genes (Fig. 6), suggesting a fundamental role in driving stem cells to differentiate into osteoblastic cells. Our results are in agreement with previous findings where BMP-2-derived peptides have been successfully tested as medium supplements for driving the osteogenic differentiation of MSCs *in vitro*.[20] Here, we showed for the first time that functionalizing HA surfaces with E7 BMP-7 modular peptides can induce osteoblastic differentiation *in vitro* using a basal medium, *i.e.*, without any osteogenic chemical or other external stimuli. Besides the biological activity due to the second domain, the self-assembly of different modular peptides at the micro-/nano-scale can also play a role in piloting the cell differentiation.[42,43] Further experiments will be necessary for a better understanding of these distinct aspects (*e.g.*, micro-/nano-architecture due to self-assembly and biological activity of the BMP-7 sequence).

## Conclusions

We envision that a modular peptide-based functionalization method can be translated to 3-D HA-based implants in the future for improving bone formation in clinical orthopaedic applications. As shown by a recent work on commercially available growth factor-based clinical products, it is still challenging to obtain optimal delivery of such molecules *in situ*: their systemic administration often involves high doses and undesired side effects.[44] Our strategy, based on *in situ* delivery of growth factor-inspired peptides through their immobilization onto HA surfaces, (i) represents an important advantage over the systemic administration, overcoming any adverse effects and (ii) preserves the bone formation at the same time.

## Supplementary Material

Refer to Web version on PubMed Central for supplementary material.

## Acknowledgements

This work was supported by the National Institutes of Health/ National Institute of Dental and Craniofacial Research (NIH/ NIDCR) grant no. 1R01DE015633. Binding/release tests were partially performed at the Molecular Foundry and supported by the Office of Science, Office of Basic Energy Sciences, of the U.S. Department of Energy under contract no. DE-AC02-05CH11231. A.P. gratefully acknowledges Dr Ronald Zuckerman and his research group for their helpful suggestions and discussions. J.W., Y.Z., and C.M. would like to thank the financial support from the National Science Foundation (CMMI-1234957, CBET-0854414, CBET-0854465, and DMR-0847758), the National Institutes of Health (5R01HL092526 and 1R21EB015190), the Department of Defense Peer Reviewed Medical Research Program (W81XWH-12-1-0384), the Oklahoma Center for the Advancement of Science and Technology (070014 and HR11-006) and the Oklahoma Center for Adult Stem Cell Research (434003).

## Notes and references

1. Dvir T, Timko BP, Kohane DS, Langer R. Nat. Nanotechnol. 2011; 6:13–22. [PubMed: 21151110]
2. Jiang J, Papoutsakis ET. Adv. Healthcare Mater. 2013; 2:25–42.
3. Thibault RA, Mikos AG, Kasper FK. Adv. Health-care Mater. 2013; 2:13–24.
4. McBeath R, Pirone DM, Nelson CM, Bhadriraju K, Chen CS. Dev. Cell. 2004; 6:483–495. [PubMed: 15068789]
5. Engler AJ, Sen S, Sweeney HL, Discher DE. Cell. 2006; 126:677–689. [PubMed: 16923388]
6. Dalby MJ, Gadegaard N, Tare R, Andar A, Riehle MO, Herzyk P, Wilkinson CD, Oreffo RO. Nat. Mater. 2007; 6:997–1003. [PubMed: 17891143]
7. Lanniel M, Huq E, Allen S, Buttery L, Williams PM, Alexander MR. Soft Matter. 2011; 7:6501.
8. Polini A, Pisignano D, Parodi M, Quarto R, Scaglione S. PLoS One. 2011; 6:e26211. [PubMed: 22022571]
9. Kilian KA, Mrksich M. Angew. Chem., Int. Ed. 2012; 51:4891–4895.
10. Gaharwar AK, Mihaila SM, Swami A, Patel A, Sant S, Reis RL, Marques AP, Gomes ME, Khademhosseini A. Adv. Mater. 2013; 25:3329–3336. [PubMed: 23670944]
11. Higuchi A, Ling QD, Chang Y, Hsu ST, Umezawa A. Chem. Rev. 2013; 113:3297–3328. [PubMed: 23391258]
12. Lapointe VL, Fernandes AT, Bell NC, Stellacci F, Stevens MM. Adv. Healthcare Mater. 2013; 2:1644–1650.
13. Wang J, Wang L, Li X, Mao CB. Sci. Rep. 2013; 3:1242. [PubMed: 23393624]
14. Juhasz JA, Best SM. J. Mater. Sci. 2011; 47:610–624.
15. Polini A, Bai H, Tomsia AP. Wiley Interdiscip. Rev.: Nanomed. Nanobiotechnol. 2013; 5:399–410. [PubMed: 23606653]
16. Yamamuro, T.; Hench, LL.; Wilson, J. Calcium Phosphate and Hydroxylapatite Ceramics. Boca Raton, FL: CRC Press; 1990.
17. LeGeros RZ. Chem. Rev. 2008; 108:4742–4753. [PubMed: 19006399]
18. Fujisawa R, Mizuno M, Nodasaka Y, Yoshinori K. Matrix Biol. 1997; 16:21–28. [PubMed: 9181551]
19. Itoh D, Yoneda S, Kuroda S, Kondo H, Umezawa A, Ohya K, Ohyama T, Kasugai S. J. Biomed. Mater. Res. 2002; 62:292–298. [PubMed: 12209950]
20. Lee JS, Lee JS, Wagoner-Johnson A, Murphy WL. Angew. Chem., Int. Ed. 2009; 48:6266–6269.
21. Gilbert M, Shaw WJ, Long JR, Nelson K, Drobny GP, Giachelli CM, Stayton PS. J. Biol. Chem. 2000; 275:16213–16218. [PubMed: 10748043]
22. Zhu H, Cao B, Zhen Z, Laxmi AA, Li D, Liu S, Mao CB. Biomaterials. 2011; 32:4744–4752. [PubMed: 21507480]

23. Culpepper BK, Phipps MC, Bonvallet PP, Bellis SL. Biomaterials. 2010; 31:9586–9594. [PubMed: 21035181]
24. Deville S, Saiz E, Tomsia AP. Biomaterials. 2006; 27:5480–5489. [PubMed: 16857254]
25. Wang J, Yang Q, Mao CB, Zhang S. J. Biomed. Mater. Res., Part A. 2012; 100:2929–2938.
26. Yang M, Shuai Y, Zhang C, Chen Y, Zhu L, Mao CB, Ouyang H. Biomacromolecules. 2014; 15:1185–1193. [PubMed: 24666022]
27. Sawyer AA, Weeks DM, Kelpke SS, McCracken MS, Bellis SL. Biomaterials. 2005; 26:7046–7056. [PubMed: 15964067]
28. Hoang QQ, Sicheri F, Howard AJ, Yang DS. Nature. 2003; 425:977–980. [PubMed: 14586470]
29. He T, Abbineni G, Cao B, Mao CB. Small. 2010; 6:2230–2235. [PubMed: 20830718]
30. Wang F, Cao B, Mao CB. Chem. Mater. 2010; 22:3630–3636. [PubMed: 20802794]
31. Xu H, Cao B, George A, Mao CB. Biomacromolecules. 2011; 12:2193–2199. [PubMed: 21520924]
32. Lee JS, Lee JS, Murphy WL. Acta Biomater. 2010; 6:21–28. [PubMed: 19665062]
33. Lu Y, Lee JS, Nemke B, Graf BK, Royalty K, Illgen R 3rd, Vanderby R Jr, Markel MD, Murphy WL. PLoS One. 2012; 7:e50378. [PubMed: 23185610]
34. Suarez-Gonzalez D, Lee JS, Lan Levengood SK, Vanderby R Jr, Murphy WL. Acta Biomater. 2012; 8:1117–1124. [PubMed: 22154864]
35. Brounts SH, Lee JS, Weinberg S, Lan Levengood SK, Smith EL, Murphy WL. Mol. Pharmacol. 2013; 10:2086–2090.
36. Culpepper BK, Bonvallet PP, Reddy MS, Ponnazhagan S, Bellis SL. Biomaterials. 2013; 34:1506–1513. [PubMed: 23182349]
37. Greenberg Z, Chorev M, Muhlrad A, Shteyer A, Namdar-Attar N, Casap N, Tartakovsky A, Vidson M, Bab I. J. Clin. Endocrinol. Metab. 1995; 80:2330–2335. [PubMed: 7629225]
38. Kim HK, Kim JH, Park DS, Park KS, Kang SS, Lee JS, Jeong MH, Yoon TR. Biomaterials. 2012; 33:7057–7063. [PubMed: 22795855]
39. Chen C, Qiu ZY, Zhang SM, Lee IS. Chem. Commun. 2011; 47:11056–11058.
40. Choi S, Yu X, Jongpaiboonkit L, Hollister SJ, Murphy WL. Sci. Rep. 2013; 3:1567. [PubMed: 23535735]
41. Stein GS, Lian JB. Endocr. Rev. 1993; 14:424–442. [PubMed: 8223340]
42. Das RK, Zouani OF. Biomaterials. 2014; 35:5278–5293. [PubMed: 24720880]
43. Trappmann B, Gautrot JE, Connelly JT, Strange DG, Li Y, Oyen ML, Cohen Stuart MA, Boehm H, Li B, Vogel V, Spatz JP, Watt FM, Huck WT. Nat. Mater. 2012; 11:642–649. [PubMed: 22635042]
44. Shields LB, Raque GH, Glassman SD, Campbell M, Vitaz T, Harpring J, Shields CB. Spine. 2006; 31:542–547. [PubMed: 16508549]

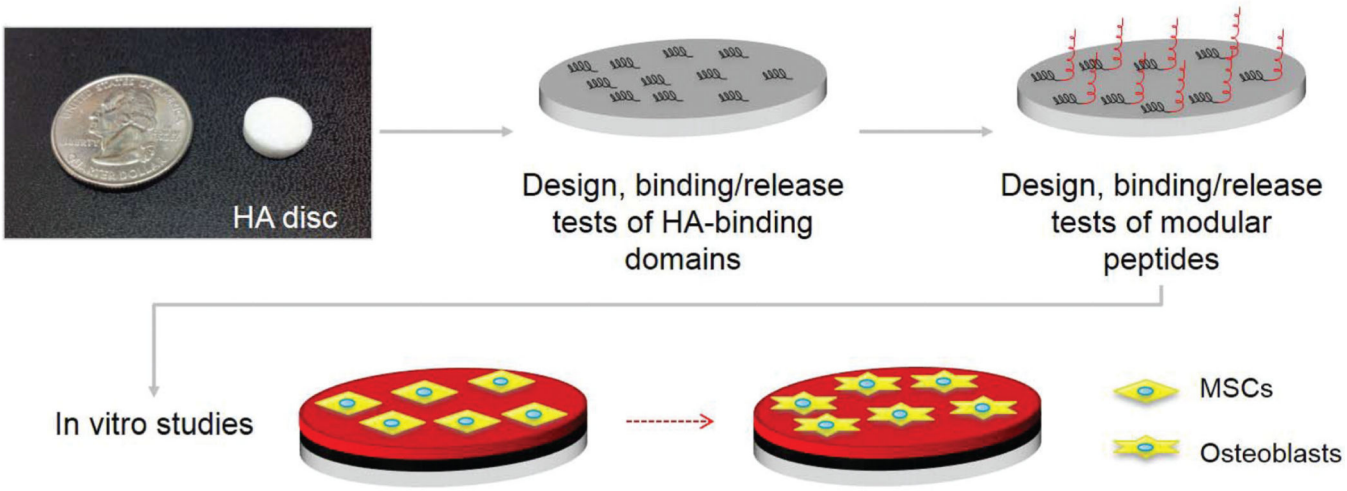


**Fig. 1.**

Overview of osteoblastic differentiation of mesenchymal stem cells (MSCs) stimulated by HA discs, functionalized with modular peptides, which are composed of two motifs including a hydroxyapatite (HA) binding sequence and a growth factor sequence as shown in Table 1.

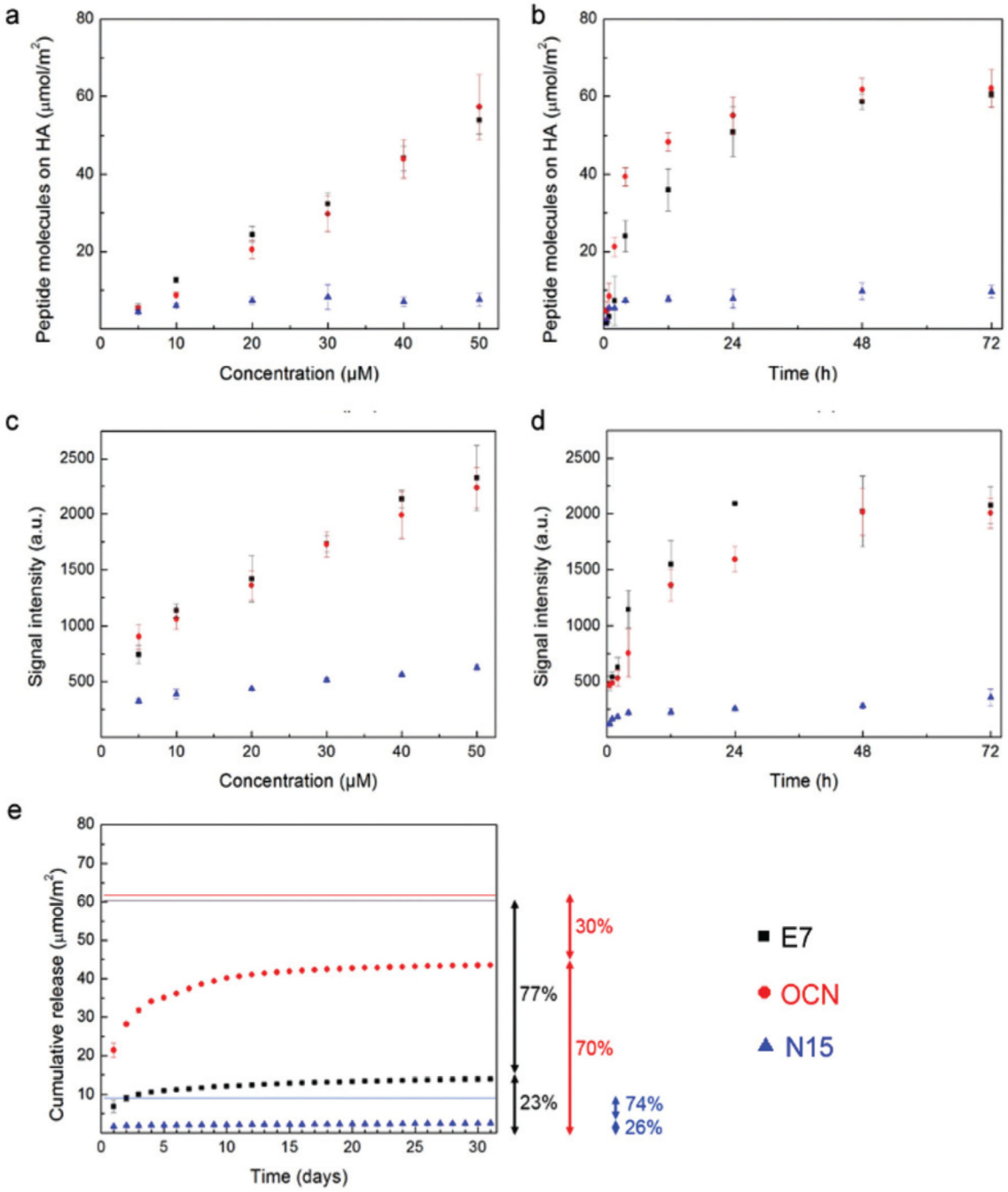


**Fig. 2.**

Binding/release tests for FITC-labeled HA-binding sequences. Binding behavior of HA-binding peptides at different concentrations (a, c) and incubation times (b, d), measured by depletion of the fluorescent signal of the coating solution (a, b) and imaging analysis (c, d). Release kinetics of HA-binding peptides (e): the continuous lines represent the 100% of peptide bound to the surface upon functionalization and are reported as reference.

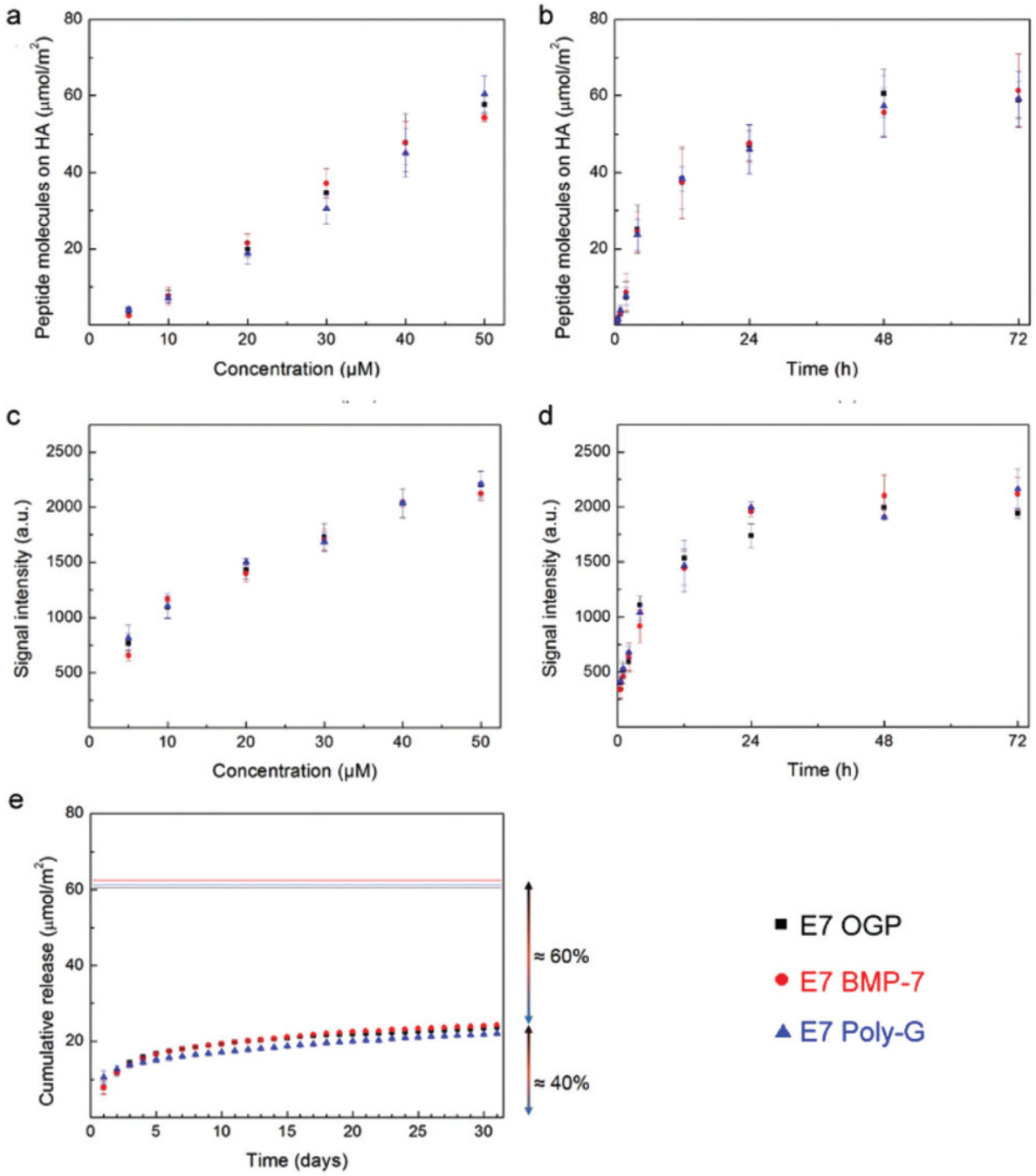


**Fig. 3.**

Binding/release tests for FITC-labeled modular peptides. Binding behaviour of modular peptides at different concentrations (a, c) and incubation times (b, d), measured by depletion of the fluorescent signal of the coating solution (a, b) and imaging analysis (c, d). Release kinetics of modular peptides (e): the continuous lines represent the 100% of peptide bound on the surface upon functionalization and are reported as reference.

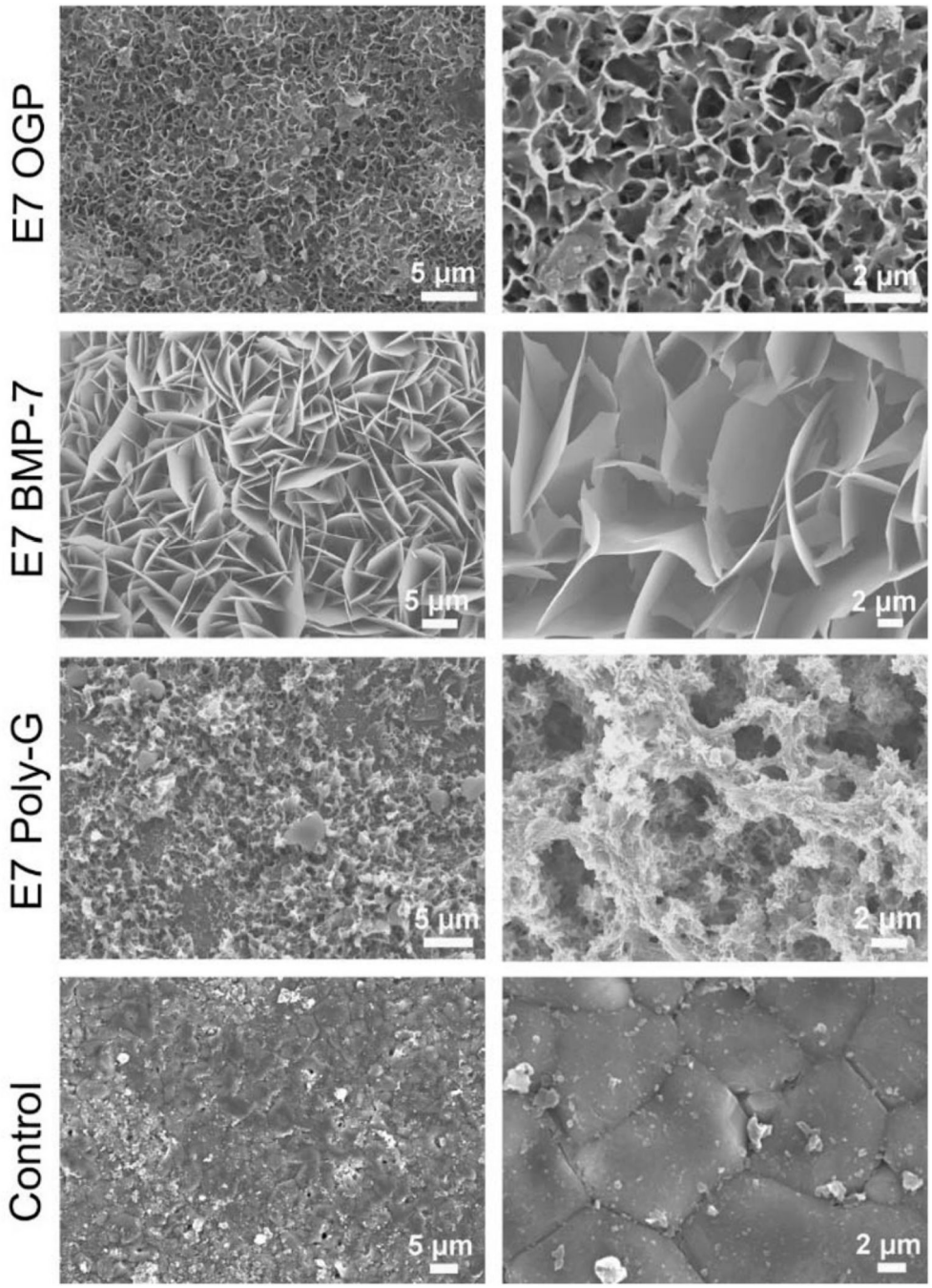


**Fig. 4.**

Surface topography derived from different functionalized modular peptides. They show different self-assembled microstructures on the HA surfaces. E7 OGP presented a porous structure and E7 BMP-7 exhibited a plate-like shape. There was no regular and uniform structure for E7 Poly-G sample. The control without any peptide coating showed salt crystals after PBS incubation.

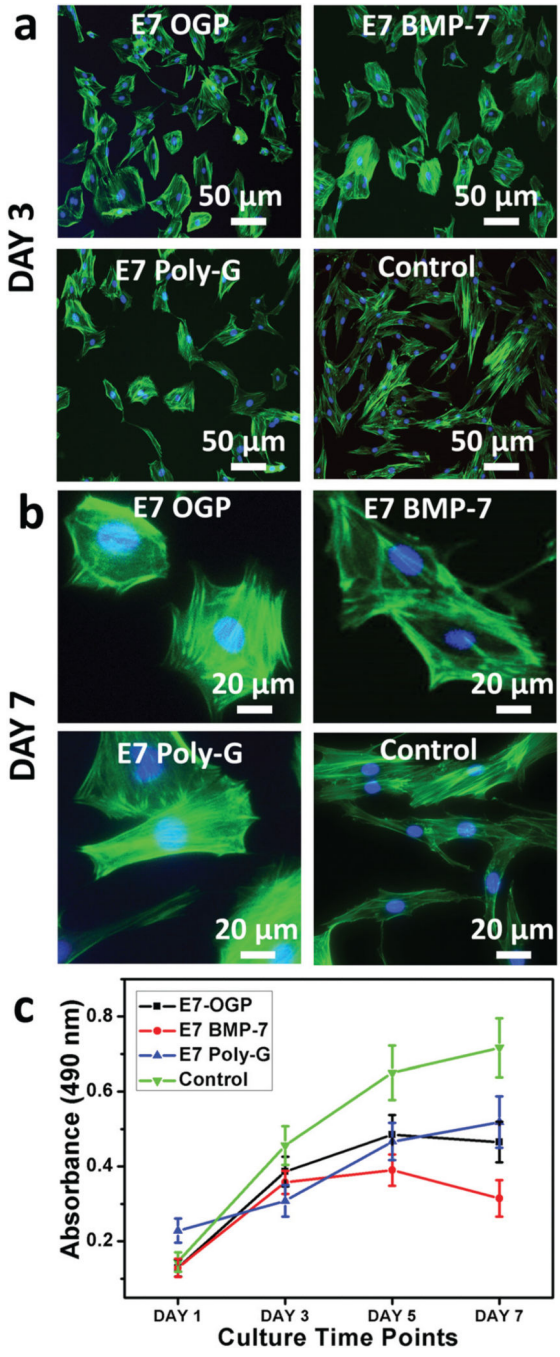


**Fig. 5.**

Cell adhesion and proliferation on different substrates. Confocal images showing cell adhesion on the different peptide-coated HA surfaces and cell proliferation after cell seeding for three days (a) and seven days (b). All materials exhibited high biocompatibility and strongly supported cell adhesion. Cells presented a significant fibroblast-like morphology in the groups of blank control and E7 Poly-G. The cell morphology changed to the broad shape in the group of E7 OGP and E7 BMP-7. Cell nuclei were stained by DAPI (blue) and F-actin

was stained by FITC-labelled phalloidin (green). Cell proliferation over time is shown (c) on the different peptide-modified discs.

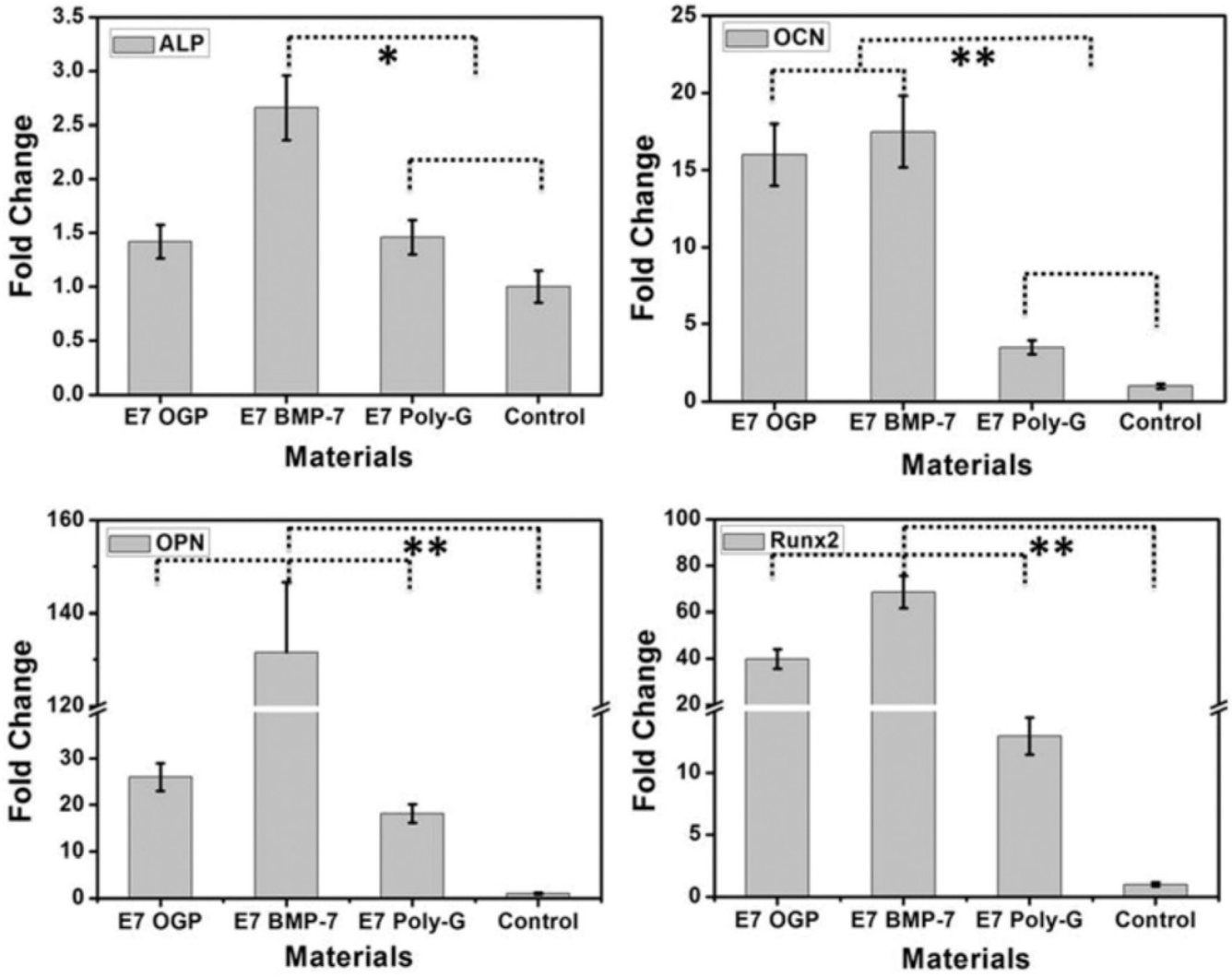


**Fig. 6.**

Real-time PCR analysis for osteogenic genes of ALP, OCN, OPN, and Runx2 after MSCs were cultured in a basal medium for three weeks. All of the osteogenic genes were overexpressed. The group of E7 BMP-7 showed higher gene expression levels of three genes than the groups of Control and E7 Poly-G. The Arbp gene was used as an internal gene and all data represented the mean ± SD ($n = 3$, $^{*}p < 0.05$, $^{**}p < 0.01$).

**Table 1**

Design of three HA-binding peptides, two modular peptides combining an E-7 HA-binding peptide and a second osteogenic peptide (derived from OGP or BMP-7), as well as a control modular peptide where the second osteogenic peptide is replaced by polyG.

| Peptide | Sequence | Peptide sources |
|---|---|---|
| E7 | EEEEEEE | BSP/ON |
| OCN | γEPRRγEVCγEL | OCN |
| N15 | DpSpSEEKFLRRIGRFG | Salivary statherin |
| E7 OGP | EEEEEEE-P-ALKRQGRTLYGFGG | BSP/ON OGP |
| E7 BMP-7 | EEEEEEE-P-GQGFSYPYKAVFSTQ | BSP/ON BMP-7 |
| E7 Poly-G | EEEEEEE-P-GGGGGGGGGGGGGGG | BSP/ON *control* |

BSP: bone sialoprotein; ON: osteonectin; OCN: osteocalcin; OGP: osteogenic growth peptide; BMP-7: bone morphogenic protein 7